HHS Public Access

Author manuscript

Neurotoxicology. Author manuscript; available in PMC 2022 June 08.

Published in final edited form as:

Neurotoxicology. 2021 September ; 86: 162–165. doi:10.1016/j.neuro.2021.08.002.

Effects of route of administration on neural exposure to platinum-based chemotherapy treatment: a pharmacokinetic study in rat

Stephen N. Housley[a,b,*], **Travis M. Rotterman**[a], **Paul Nardelli**[a], **Dario I. Carrasco**[a], **Richard K. Noel**[c], **Laura O'Farrell**[c], **Timothy C. Cope**[a,b,d,*]

[a]School of Biological Sciences, Georgia Institute of Technology, Atlanta, 30332, Georgia

[b]Integrated Cancer Research Center, Parker H. Petit Institute for Bioengineering and Bioscience, Georgia Institute of Technology, 315 Ferst Drive, Atlanta, GA, 30309, USA

[c]Physiological Research Laboratory, Georgia Institute of Technology, Atlanta, GA, USA

[d]W.H. Coulter Department of Biomedical Engineering, Emory University and Georgia Institute of Technology, Georgia Institute of Technology, Atlanta, 30332, Georgia

Abstract

The persisting need for effective clinical treatment of chemotherapy-induced neurotoxicity (CIN) motivates critical evaluation of preclinical models of CIN for their translational relevance. The present study aimed to provide the first quantitative evaluation of neural tissue exposed *in vivo* to a platinum-based anticancer compound, oxaliplatin (OX) during and after two commonly used dosing regimens: slow IV infusion used clinically and bolus IP injection used preclinically. Inductively-coupled plasma mass spectrometry analysis of dorsal root ganglia indicated that while differences in the temporal dynamics of platinum distribution exist, key drivers of neurotoxicity, e.g. peak concentrations and exposure, were not different across the two routes of administration. We conclude that the IP route of OX administration achieves clinically relevant pharmacokinetic exposure of neural tissues in a rodent model of CIN.

Keywords

Chemotherapy-induced neurotoxicity; Dorsal root ganglia; Oxaliplatin; Massspectrometry; Preclinical validation

[*]Corresponding authors at: School of Biological Sciences, Georgia Institute of Technology, Atlanta, 30332, Georgia. nickhousley@gatech.edu (S.N. Housley), tim.cope@gatech.edu (T.C. Cope).

Author contributions

T.C.C and S.N.H. designed, directed and coordinated this study. S.N. H., P.N., T.M.R., D.I.C., L.O., R.K.N. performed the experiments. S.N.H. designed and implemented analyses. S.N.H., T.C.C wrote the manuscript.

Declaration of Competing Interest

The authors declare that they have no known competing financial interests or personal relationships that could have appeared to influence the work reported in this paper.

1. Introduction

Chemotherapy-induced neurotoxicity (CIN) is a constellation of time-varying signs and symptoms that negatively impact the perception and function of cancer survivors treated by chemotherapy. Preclinical models have been utilized for decades to develop mechanistic understanding of CIN that is not feasible in clinical populations. To optimize translational relevance, preclinical models should reliably simulate clinical disease and treatment. Among the factors that play a role in generalizing results from animal models to patients are treatment dosing parameters. For example, the frequency and cumulative dose contribute to the development of CIN preclinically (Cavaletti et al., 2001) and clinically (de Gramont et al., 2000; Grothey, 2021). The route of administration is another important dosing characteristic that has the potential to influence translational relevance, but has yet to be formally evaluated for neural tissues involved in CIN.

Slow intravenous (IV) infusion, lasting 2 h or more, is the standard-of-care for platinum-based chemotherapies (PBCs) (Ibrahim et al., 2004), whereas bolus intraperitoneal (IP) injections are frequently used preclinically, secondary to its experimental simplicity. Potential differences in systemic and tissue exposure to PBCs has led to questions about the comparability of IP and IV routes of administration (Bruna et al., 2020). While IP and IV routes of administration have been directly compared in preclinical models (Pestieau et al., 2001), measures centered on serum and IP fluid concentration of PBCs. Consequently, this has indirect relevance to the development of CIN, which is attributed to preferential targeting of peripheral nervous system, chiefly the dorsal root ganglia (DRG) by various PBCs such as oxaliplatin (OX). Inferences drawn from this study are further complicated due to the selection of a bolus IV dosing strategy, which does not model the pharmacokinetics of slow IV infusion used clinically (Graham et al., 2000). Bolus IV injections rapidly expose circulation to large amounts of chemotherapy and are associated with increased probability of systemic toxicities (Pestieau et al., 2001), consequences that are avoided through slow infusion.

There is no information on the exposure of DRG to PBC following the clinically-relevant slow IV infusion, nor is it known how closely IP injections model slow IV infusion for the tissues of interest in CIN. Identifying the most appropriate dosing regimen is critical to establish and validate future preclinical models and for contextualizing inferences drawn from previous preclinical studies. The present study provided the first neural tissue specific (DRG) characterization of slow IV infusion of OX and provide the first quantitative comparison with an IP dosing regimen. The IP route of administration approximated key characteristics of slow IV infusion such as peak concentrations and total exposure, despite nominal differences in the temporal distribution of OX. We conclude that the IP route of administration is a valid method to deliver clinically relevant doses of OX to neural tissues in preclinical models.

2. Methods

2.1. Animals and treatments

Procedures and experiments were approved by the Georgia Institute of Technology Institutional Animal Care and Use Committee. Animals were housed in individually ventilated cages and provided food (Lab-Diet® 5001) and water ad libitum in a temperature- and light-controlled environment with lights on and off at 0700 and 1900 respectively. Experiments were conducted between 0900 and 1600. Each animal was euthanized by isoflurane overdose combined with exsanguination.

Fifty-six adult (250–350 g) Fisher 344 (F344) rats were randomly assigned to receive either IP injection or slow IV infusion. Both groups received 10 mg/kg of OX (ThermoFisher: Acros Organics™) in 1.5 mL of 5 % dextrose (Baxter Healthcare Corporation) resulting in a 6.67 mg/mL final concentration. IP injection procedures have been described previously (Housley et al., 2020a, b). Slow IV infusions were delivered through a cannulated right external jugular vein (O'Farrell et al., 1996) using an infusion pump (New Era Pump Systems, Inc or Kent Scientific GenieTouch) set at a continuous rate of 0.75 mL/1 h for 2 h. The external jugular vein was exposed with a small longitudinal incision (1 cm) just right of midline followed by blunt dissection of the surrounding muscle, connective tissue, and fat. Curved forceps were inserted under the vein to aid placement of two ligatures, one superior and one inferior to the cannulation site. The superior ligature was then tightened. A small 0.5 mm ovoid incision was made on the ventral aspect of the vein thus maintaining the dorsal aspect in continuity. A smooth tip silicone - tube (0.20 in ID, 0.037 in OD S/P Medical Grade, Baxter Scientific, McGaw Park, IL) canula was inserted in the opening progressed between 18–20 mm proximally toward the right atrium. Patency was confirmed by blood draw into the exposed cannula after whjch the cannula was flushed with 1 mL of 5% dextrose. After insertion, the proximal ligature was tightened around the circumference of the vein and the inserted silicone cannula. Animals were either studied acutely at predetermined time points (described below) or 72 h following OX injections (long-term).

For acute studies (n = 48), rats were deeply anesthetized, first induced by brief inhalation of isoflurane (5% in 100 % O2), and then maintained throughout the remainder of the experiment via a tracheal cannula (1.5–2.5 % in 100 % O2). Vital signs were continuously monitored including, core temperature (36–38 °C), PCO2 (3–5 %), respiratory rate (40–60 breaths/min), pulse rate (300–450 bpm) and SPO2 (>90 %). Animals remained anesthetized for the entirety of the experiment until DRG harvest, ranging from 30–270 min (Fig. 1).

For long-term studies (n = 8), rats were deeply anesthetized by inhalation of isoflurane (5% in 100 % O2), and maintained on nose cone (1.5–2.5 % in 100 % O2 for a maximum of 3 h). Sterile surgical procedures were used to place the cannula as described above. After drug delivery, the cannula was removed, the wound was closed, and anesthesia was discountinued. A single sustained release buprenorphine (Zoopharm, Windsor, CO) dose (0.05–0.10 mg/kg) was injected subcutaneously for postsurgical pain management. All animals were monitored daily for surgical complications or signs of distress. No

postinjection pain management was required for long-term studies following IP injection (n = 4, Fig. 1).

2.2. DRG extraction

Eight lumbosacral DRG were harvested from four animals per group via laminectomy at one of the 7 randomly assigned endpoints: 5, 30, 60, 120, 180, 240 min, and 72 h after OX injection. This afforded quantification of the concentration of OX through its metal constituent platinum (Pt) in DRG at various times during or after infusion completion (Fig. 1). After DRG extraction, rats were euthanized with isoflurane overdose followed by exsanguination. Following euthanasia, all cannulas were removed and inspected. We found that all tubing was intact.

2.3. Determination of DRG platinum concentration

Blinded investigators quantified Pt concentration in DRG through inductively coupled plasma mass spectrometry (ICP-MS) analysis. ICPMS is the gold standard for heavy metal quantification in trace amounts and was chosen because of its superior sensitivity compared to other available techniques for the detection of Pt in tissues (Wilschefski and Baxter, 2019). Previously validated standard biological sample digestion and preparation were used in accordance with EPA Method 3052 and standard ICP/MS analytic techniques were used in accordance with EPA Method 200.8 and are briefly described below.

Pooled DRG were transferred to 120 mL teflon digestion vessels, followed by the addition of 3 mL of nitric acid for sample digestion. After 30 min, vessels were placed in a microwave oven (1000 W) for 10 min at power level 40 %, then for another 15 min at power level 30 %. 8 samples were prepared at a time. The digested samples were reconstituted by addition of 5 mL of double deionized water for ICP/MS analysis. Prior to ICP/MS analysis the samples were diluted 1:1 with 0.5 % of Sodium hydroxide. The Elan 9000 (Perkin Elmer-Sciex) ICP-MS equipped with an AS 91 auto-sampler (PerkinElmer, Norwalk, CT, USA) was used for Pt analysis. The instrument conditions used were: FR power—1100 W, nebulizer gas flow (L/min)—0.90. Measuring conditions: scan mode—peak hopping, dwell time—50 ms, sweeps—40, integration time—2000 ms. The sensitivity (detection limit) for Pt under this method is 0.1 to 0.5 ng/L. The linearity was up to 100 ppm, with a relative standard deviation less than 2 %. Standards were obtained from Perkin Elmer, Inc. (Branford, CT, USA). All analyses took place in a single batch so no batch drift correction was required.

2.4. Data analysis

We quantified the Pt concentration in DRG in four animals per group (IV and IP). From each animal, eight lumbosacral DRG were divided and pooled into two biologic replicates per animal (e.g. 2 replicates per animal containing 4 DRG each). Summary statistics of observed data are reported as mean ± SD (Table 1). Because repeated measures were not possible, single time points were concatenated across animals to estimate the total area under the curve ($AUC_{(tDRG)}$) to the last time point and hourly exposure of the DRG. In this way, we generated 8 constructed time courses for each experimental condition (IP and

IV). $AUC_{(tDRG)}$ and total exposure were calculated using the AUC spline and trapeziod interpolation rule in the package *DescTools* in R (4.0.3) (Team, R. C., 2018).

We utilized a fully Bayesian Generalized Additive Mixed Model (GAMM) that utilizes group-specific terms and includes nonlinear functions of predictors called “smooths”. So-called “thin-plate splines” are used to model Pt concentration in DRG over time (k = 6). We also specify a group-specific time-by-route term as a one-sided formula that is passed to the random argument. The GAMM allows smooth components to be estimated for time and route of administration using stan_gamm4 function from the rstanarm package. All data were logtransformed prior to analysis. General modeling and validation techniques have been described in previously published reports from this laboratory (Housley et al., 2020a, b; Horstman et al., 2019). Briefly, Bayesian parameter estimation was used to derive the entire joint posterior distribution of all parameters simultaneously for statistical comparison. Highest (posterior) density interval (HDI) was used to make unbiased inferences by directly comparing the posterior probability distributions (95 %) between two contrasts of interests e.g. mean-comparisons testing of Pt concentration over a specific time (Housley et al., 2020a; Horstman et al., 2019). All models were developed with the *rstanarm* package (2.21.1) (Gabry and Goodrich, 2018) in R (4.0.3) (Team, R. C., 2018). Models were validated by computing out-of-sample predictive accuracy using Pareto-smoothed importance sampling (PSIS (Vehtari et al., 2017)) to perform leave-one-out cross validation as previously described (Housley et al., 2020a, b).

3. Results

ICP-MS quantification of Pt in DRG by route of administration (n = 2) and time (n = 7) are reported in Table 1. IP route of administration achieved peak, stable Pt values 60 min after bolus injection, whereas IV route of administration achieved peak stable Pt values 120 min after initiation of slow infusion, the time when the full dose was delivered (Table 1). These data indicate that Pt distributes slowly after IP administration despite a bolus injection. The slow distribution mirrors that achieved by experimentally restricting the dose through slow infusion, likely reflecting a slow release to systemic circulation from the IP fluid in agreement with previous reports (Pestieau et al., 2001).

We then modeled the rate of Pt distribution in DRG (see Methods) to test for statistical differences. Inspection of the HDI of the posterior predictive distributions over time, between groups, revealed small but significant differences in initial Pt values and final concentration; however, we find no difference in the peak Pt concentration (Fig. 2). To understand the overall exposure of DRG to Pt, we calculated the time-averaged $AUC_{(tDRG)}$ (Methods). Fig. 3 shows the $AUC_{(tDRG)}$ IP: 620.36 ± 68.72 vs. IV: 606.32 ± 65.29 μgh•/m using the quadratic spline interpolation method which corresponds tightly with $AUC_{(tDRG)}$ calculated using the trapezoid method IP: 610.77 ± 64.94 vs. IV: 612.38 ± 68.61 μg•h/mL. Inspection of the posterior predictive distributions for each route of administration revealed substantial overlap, indicating that a non-significant difference in time averaged Pt exposure of −14.6 μg h/mL (95 %HDI: −213 to 176). Further inspection of the posteriors allows estimation of T_{max} and C_{max} values for both routes of administration. While T_{max} occurs earlier following IP injection, 128.37 min as compared to 192.61 min for slow infusion IV,

C_{max} values were not different (IV: 95 %HDI: 6.28–21.87 ppm and IP 95 %HDI: 6.50–20.89 ppm). Data were transformed back from log scale for interpretation.

4. Discussion

We present the first quantitative evaluation of the temporal exposure of DRG to PBC during and after two dosing regimens: clinically relevant slow IV infusion and preclinically common IP injection. The data indicate that while statistical differences in the temporal dynamics of Pt distribution exist, peak concentrations and exposure were not different across the two routes of administration. Based on previous work (Grolleau et al., 2001; Adelsberger et al., 2000), the differences we observe between IP injection and IV infusion (<10 ppm) will minimally affect the DRG exposure to PBCs. For example, a previous study made by Grolleau et al. (Grolleau et al., 2001) using direct application through patch clamp electrodes to cultured ganglion neurons from cockroach CNS and by Adelsberger et al., 2000 using bath application to rat ex vivo nerve preparations detected effects on sodium channel function that were approximately 10–25 times higher than the levels observed in the present study. A more recent study agreed with these inferences after finding a left shift in voltage-dependence of sodium conductance in A-Fiber DRG neurons after 10 min of 100 μM (39.7 ppm) oxaliplatin (Lee et al., 2020). These and other comparisons with previous studies (Cavaletti et al., 2001) in addition to the clinical evidence indicating cumulative dose/exposure were most predictive (Saif and Reardon, 2005; Grothey, 2005), suggest that the temporal differences in concentrations observed between IP and IV delivery of OX will minimally affect the DRG exposure to PBCs.

4.1. Data driven preclinical model recommendation

Data from this study support the utility of the IP route of administration for preclinical studies of CIN. Its simplicity and reproducibility in application as well as its comparability to the clinically relevant slow IV infusion route endow substantial advantages over alternative methods, e.g. bolus tail vein injection and even the slow IV infusion method utilized here. These advantages are amplified in the context of studying chronic CIN wherein repeated doses, e.g. 5–10 are required to achieve clinical relevance. Chronic slow infusion systems are available but present substantial challenges such as cost and complications associated with surgical implantation and maintenance (patency, infection risk) of indwelling systems. Instead, we suggest that the IP route of administration be adopted for future preclinical models of CIN. However, IP dosing is not without complications. Investigators wishing to adopt this method should be vigilant to potential consequences such as local inflammatory responses (fibrinopurulent peritonitis) (Cavaletti et al., 2001) and inaccurate delivery (Lewis, 1966). Both risks can be mitigated by less frequent IP injections, e.g. once instead of twice per week (Cavaletti et al., 2001), and tissue specific validation of PBC delivery, e. g. ICP-MS. Additional considerations should be given to define the optimal translational model such as frequency (Cavaletti et al., 2001), cumulative dose (Cavaletti et al., 2001; de Gramont et al., 2000; Grothey, 2021) and the presence of cancer (Housley et al., 2020a) all of which have documented roles in the development of CIN.

Acknowledgments

We thank Dr. Sayed Hassan at the University of Georgia's Center for Applied Isotope Studies. This work is supported by NIH grant R01CA221363 and Northside Hospital Foundation, Inc.

References

Adelsberger H, et al. , 2000. The chemotherapeutic oxaliplatin alters voltage-gated Na+ channel kinetics on rat sensory neurons. Eur. J. Pharmacol 406, 25–32. [PubMed: 11011028]

Bruna J, et al. , 2020. Methods for in vivo studies in rodents of chemotherapy induced peripheral neuropathy. Exp. Neurol 325, 113154. [PubMed: 31837318]

Cavaletti G, et al. , 2001. Effects of different schedules of oxaliplatin treatment on the peripheral nervous system of the rat. Eur. J. Cancer 37, 2457–2463. [PubMed: 11720843]

de Gramont Ad., et al. , 2000. Leucovorin and fluorouracil with or without oxaliplatin as first-line treatment in advanced colorectal cancer. J. Clin. Oncol 18, 2938–2947. [PubMed: 10944126]

Gabry J, Goodrich B, 2018. Rstanarm: Bayesian Applied Regression Modeling Via Stan. R Package Version 2.18.1.

Graham MA, et al. , 2000. Clinical pharmacokinetics of oxaliplatin: a critical review. Clin. Cancer Res 6, 1205–1218. [PubMed: 10778943]

Grolleau F, et al. , 2001. A possible explanation for a neurotoxic effect of the anticancer agent oxaliplatin on neuronal voltage-gated sodium channels. J. Neurophysiol 85, 2293–2297. [PubMed: 11353042]

Grothey A, 2005. Clinical management of oxaliplatin-associated neurotoxicity. Clin. Colorectal Cancer 5, S38–S46. [PubMed: 15871765]

Grothey A in Proc Am Soc Clin Oncol. 129a.

Horstman GM, Housley SN, Cope TC, 2019. Dysregulation of mechanosensory circuits coordinating the actions of antagonist motor pools following peripheral nerve injury and muscle reinnervation. Exp. Neurol

Housley SN, et al. , 2020a. Cancer exacerbates chemotherapy-induced sensory neuropathy. Cancer Res.

Housley SN, Nardelli P, Powers RK, Rich MM, Cope TC, 2020b. Chronic defects in intraspinal mechanisms of spike encoding by spinal motoneurons following chemotherapy. Exp. Neurol 113354. [PubMed: 32511953]

Ibrahim A, et al. , 2004. FDA drug approval summaries: oxaliplatin. Oncologist 9, 8–12. [PubMed: 14755010]

Lee JH, Gang J, Yang E, Kim W, Jin Y-H, 2020. Bee venom acupuncture attenuates oxaliplatin-induced neuropathic pain by modulating action potential threshold in a-fiber dorsal root ganglia neurons. Toxins 12, 737.

Lewis R, 1966. Error of intraperitoneal injections in rats. Lab. Anim. Care 16, 505–509. [PubMed: 4291449]

O'Farrell L, Griffith JW, Lang CM, 1996. Histologic development of the sheath that forms around long-term implanted central venous catheters. J. Parenter. Enter. Nutr 20, 156–158.

Pestieau SR, Belliveau JF, Griffin H, Stuart OA, Sugarbaker PH, 2001. Pharmacokinetics of intraperitoneal oxaliplatin: experimental studies. J. Surg. Oncol 76, 106–114. [PubMed: 11223836]

Saif MW, Reardon J, 2005. Management of oxaliplatin-induced peripheral neuropathy. Ther. Clin. Risk Manag 1, 249. [PubMed: 18360567]

Team, R. C. (ISBN 3-900051-07-0: URL http://www.R-project.org, 2018).

Vehtari A, Gelman A, Gabry J, 2017. Practical Bayesian model evaluation using leave-one-out cross-validation and WAIC. Stat. Comput 27, 1413–1432.

Wilschefski SC, Baxter MR, 2019. Inductively coupled plasma mass spectrometry: introduction to analytical aspects. Clin. Biochem. Rev 40, 115. [PubMed: 31530963]

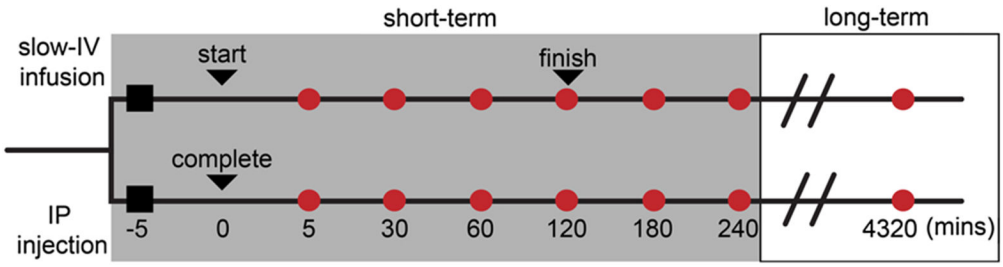

Fig. 1.

Experimental design and dosing timeline. Rats assigned using block randomization (to ensure equal group membership) received either slow-IV infusion (referred to as IV) or IP injection for a specific terminal tissue collection (time frames indicated by circles along each experimental path). Black squares indicate start of experiment and induction of anesthesia. For IV study path (top line) the first black triangle indicates the start of infusion. The second black triangle indicates the completion (i.e. full dose delivered). For the IP study path (bottom line), the only triangle indicates the time at which full dose is delivered. For the short-term studies (grey box), all animals remain anesthetized until the specific terminal tissue collection time is reached (red circle). Four (4) animals were allocated to each red circle, for each of the two paths (IV and IP). Animals randomly assigned to the long-term study (white box), were removed from anesthesia (as detailed in Methods) following IV or IP dosing and allowed to survive for 72 h (4320 min) for terminal tissue collection (n = 4 per study path).

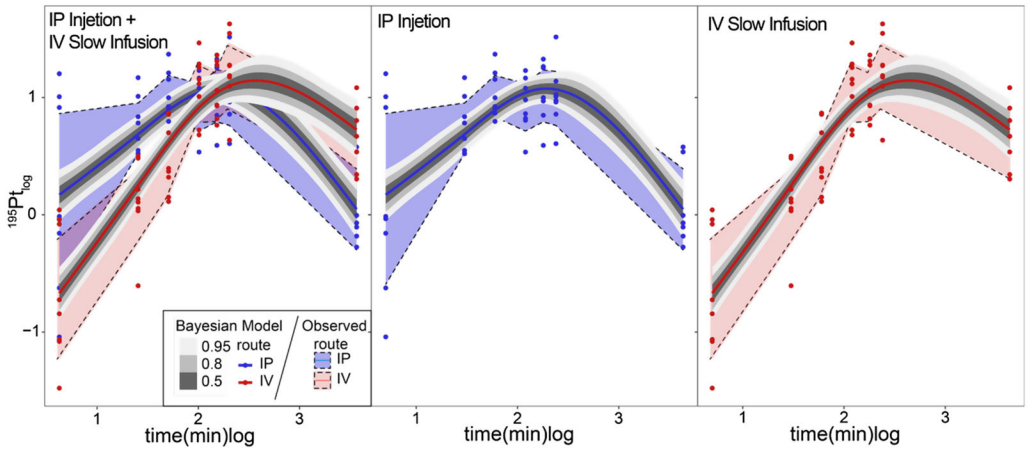

Fig. 2.

Modeling temporal by route of administration dynamics of platinum distribution in dorsal root ganglia. Bayesian generalized additive mixed modeling predictions of the rate of platinum distribution in dorsal root ganglia for both intraperitoneal and intravenous injection methods. Posterior predictive intervals (50 %, 80 % and 95 % highest density intervals in grey scale) for both routes (smoothed trajectories) superimposed on observed distributions (left most plot). Middle and right plots show parsed modeling and observed distributions for ease of comparison. Data were $\log_{10}$-transformed for all analysis and presented on $\log_{10}$-scale.

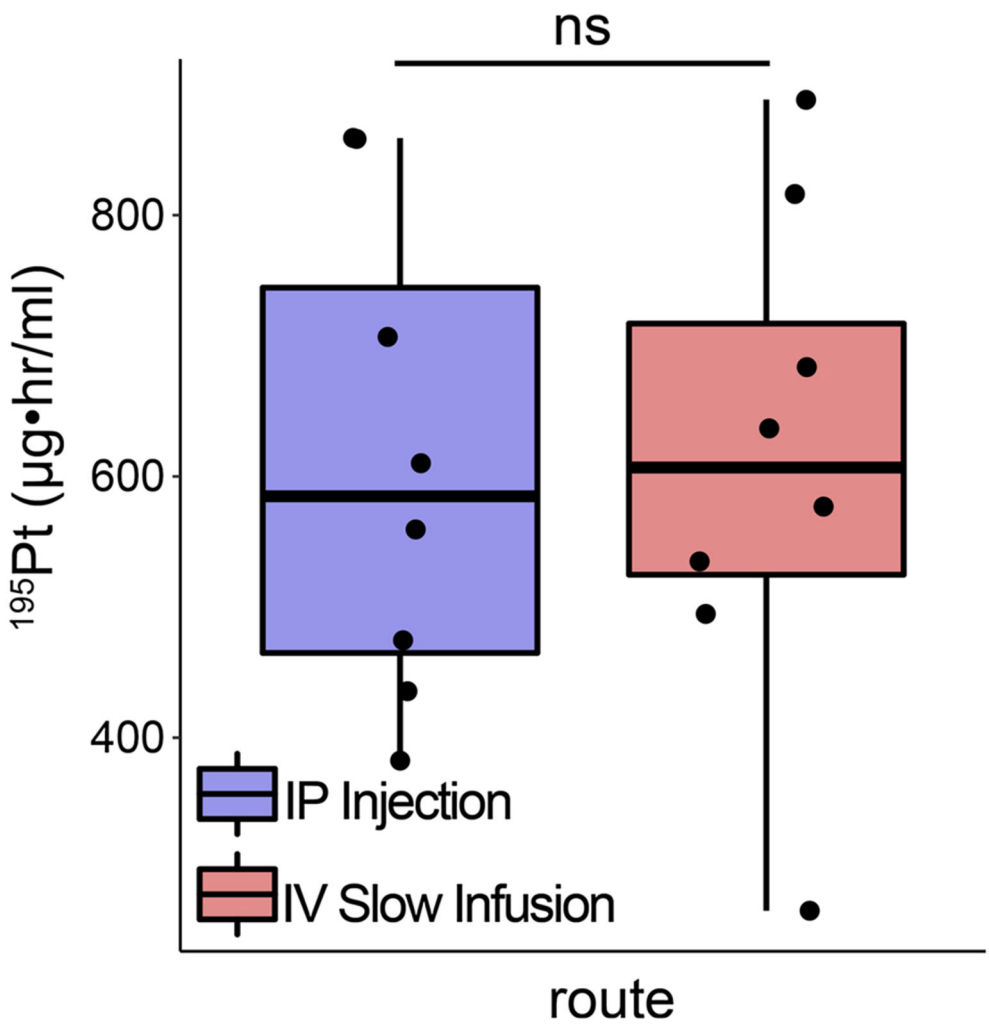

Fig. 3.

Time averaged exposure of dorsal root ganglia to platinum does not differ between routes of administration. Quantification of modeled time courses for each experimental condition. Time averaged exposures were calculated using the spline interpolation rule. ns - indicates no statistically significant comparisons were detected as empirically derived from hierarchical Bayesian model (stan_glm): 95 % highest density intervals do not overlap.

Table 1

Observed ICP-MS quantification of Pt in DRG by route of administration.

DRG Pt concentrations	***IP (ppm)***			***IV (ppm)_***		
Time point	***Mean***	***Std. Dev.***	***SEM***	***Mean***	***Std. Dev.***	***SEM***
5 (min)	4.65	6.01	2.13	0.422	0.44	0.17
30 (min)	6.57	4.07	1.43	1.62	1.00	0.35
60 (min)	11.75	5.85	2.07	3.65	2.51	0.89
120 (min)	9.62	4.61	1.63	14.29	8.03	2.84
180 (min)	12.22	6.17	2.18	12.95	6.83	2.42
240 (min)	12.15	8.81	3.11	20.326	12.47	4.41
72 (hrs) (long-term)	1.58	1.40	0.53	5.56	3.64	1.38

Acute and long-term pattern of platinum distribution in dorsal root ganglia. Average platinum concentration (n = 4 rats per experimental group) with two biologic replicates each at all the observed time points (n = 7).